PAPER

Improving the electrical contact at a Pt/TiO_2 nanowire interface by selective application of focused femtosecond laser irradiation

To cite this article: Songling Xing *et al* 2017 *Nanotechnology* **28** 405302

View the article online for updates and enhancements.

Related content

- Resistance switching in oxides with inhomogeneous conductivity
  Shang Da-Shan, Sun Ji-Rong, Shen Bao-Gen et al.
- Significantly enhanced visible light response in single TiO2 nanowire by nitrogen ion implantation
  Pengcheng Wu, Xianyin Song, Shuyao Si et al.
- Ultraviolet detection using TiO2 nanowire array with Ag Schottky contact
  P Chinnamuthu, J C Dhar, A Mondal et al.

This content was downloaded from IP address 129.97.36.3 on 19/03/2018 at 15:49

IOP Publishing Nanotechnology
Nanotechnology 28 (2017) 405302 (8pp) https://doi.org/10.1088/1361-6528/aa8150

Improving the electrical contact at a Pt/TiO_2 nanowire interface by selective application of focused femtosecond laser irradiation

Songling Xing[1], Luchan Lin[1], Guisheng Zou[1], Lei Liu[1], Peng Peng[2], Aiping Wu[1], Walter W Duley[3] and Y Norman Zhou[1,3]

[1] Department of Mechanical Engineering, State Key Laboratory of Tribology, Tsinghua University, Beijing 100084, People's Republic of China
[2] School of Mechanical Engineering and Automation, International Research Institute for Multidisciplinary Science, Beihang University, Beijing 100191, People's Republic of China
[3] Centre for Advanced Materials Joining, University of Waterloo, Waterloo, Ontario N2L 3G1, Canada

E-mail: liulei@mail.tsinghua.edu.cn

Received 5 June 2017, revised 18 July 2017
Accepted for publication 21 July 2017
Published 12 September 2017

Abstract

In this paper, we show that tightly focused femtosecond laser irradiation is effective in improving nanojoining of an oxide nanowire (NW) (TiO_2) to a metal electrode (Pt), and how this process can be used to modify contact states. Enhanced chemical bondings are created due to localized plasmonically enhanced optical absorption at the Pt/TiO_2 interface as confirmed by finite element simulations of the localized field distribution during irradiation. Nano Auger electron spectroscopy shows that the resulting heterojunction is depleted in oxygen, suggesting that a TiO_{2-x} layer is formed between the Pt electrode and the TiO_2 NW. The presence of this redox layer at the metal/oxide interface plays an important role in decreasing the Schottky barrier height and in facilitating chemical bonding. After laser irradiation at the cathode for 10 s at a fluence of 5.02 mJ cm^{-2}, the Pt/TiO_2 NW/Pt structure displays different electrical properties under forward and reverse bias voltage, respectively. The creation of this asymmetric electrical characteristic shows the way in which modification of the electronic interface by laser engineering can replace the electroforming process in resistive switching devices and how it can be used to control contact states in a metal/oxide interface.

Keywords: femtosecond laser, interface modification, plasmonic effect, TiO_2 nanowire

(Some figures may appear in colour only in the online journal)

1. Introduction

Research on functional nanodevices based on nanomaterials involves many areas of physical and chemical science [1–4]. The possibility of unique structures combined with the excellent performance of nanowire (NW)-based materials have attracted much interest because device development is driven by the continuous demand for miniaturization, low power consumption, low cost and high reliability [5–7]. An additional advantage is that semiconductor NWs with tailored chemical composition and electronic properties [8, 9] can be assembled into functional electronic, chemical and photonic devices, such as single NW field-effect transistors [10], water-splitting system [11], nanoscale LEDs [12] and plasmon-enhanced lasers [13]. Since TiO_2 is a representative metal-oxide-semiconductor with a wide band gap [14] and a high recombination rate for photoinduced electrons and holes [15, 16], it has been widely used as a component in the fabrication of functional devices. The properties of TiO_2 are dependent on microstructure and crystallographic phase, which can be controlled by structural modification to enhance device performance [17].

The nature of the contact at the interface between metal and semiconductor can determine the overall performance of functional devices based on these materials. For example, to obtain a fast-response ultraviolet detector incorporating a p–n

 © 2017 IOP Publishing Ltd Printed in the UK

junction, an Ohmic contact, transformed from a Schottky contact, between metal electrode and a semiconductor NW has been fabricated to enhance the current response [18]. Because of the functional demands of nanoscale devices, the challenges involved in changing the contact at an interface contact mostly relate to obtaining a reliable, localized and cost-effective process. Ohmic contacts can be achieved by direct deposition of Pt followed by welding the metal to the semiconductor using a focused ion beam. However, this method is costly [19]. Other techniques, such as chemical processing and photolithography, are not compatible with a simple accurate deposition process [20, 21]. An alternative is provided by engineering with femtosecond (fs) laser irradiation as this combines the controlled input of localized energy, ultrashort pulse width, extremely high peak intensity and operation in air [22]. In addition, focusing the fs laser beam introduces strong absorption in highly localized regions, and contributes to the trapping of plasmons at the metal–semiconductor interface [23]. Both processes open up new fabrication technologies in the fabrication of nanodevices.

In this paper we report a new method, based on nanoscale fs laser processing, for modifying contact states at the Pt/TiO_2 NW interface. Simulations show that strong enhancement of the dynamic electric field occurs at the metal/oxide interface under fs laser irradiation which results in the formation of heterojunctions. The relative concentrations of surface oxygen in and around the fs laser-induced region have been measured, and indicate that a redox layer is formed at the junction. The electrical response and the mechanism of this laser-induced effect and its possible applications in the engineering of new devices are also discussed.

2. Experimental section

TiO_2 NWs were synthesized using a method developed in a previous study [24]. 60 ml NaOH alkaline solution (10 M) in a 125 ml Teflon-lined stainless steel autoclave (Parr Instruments) was used to dissolve 2 g of P25 AeroxideTM (Evonik Industries AG) as TiO_2 source. The solution was then kept in a furnace for the growth of $Na_2Ti_3O_7$ at 190 °C for 72 h. After cooling the reactor, the suspended NWs were transferred into 100 ml conical tubes and centrifuged five times using Millipore water. Subsequently, the NWs were transferred into 0.1 M HCl solution for an ion exchange process where $H_2Ti_3O_7$ solution was obtained. After filtration, $H_2Ti_3O_7$ was dried in a furnace at 80 °C for 8 h. Finally, the products were annealed at 900 °C for 2 h.

Pt/Ti electrodes incorporating a 2 μm finger spacing were fabricated by optical lithography and lift-off process on oxidized Si substrate (300 nm SiO_2). The thicknesses of Pt (up) and Ti (bottom, as a connection between Pt and SiO_2) layers are 200 nm and 5 nm respectively. Figure 1 shows the process of assembling the bridged Pt/TiO_2 NW/Pt structure by depositing the NW on the electrodes. Firstly, the TiO_2 NW powder was dispersed and diluted in a high-purity acetone solution. The solution was then drop-cast on a chip with Pt

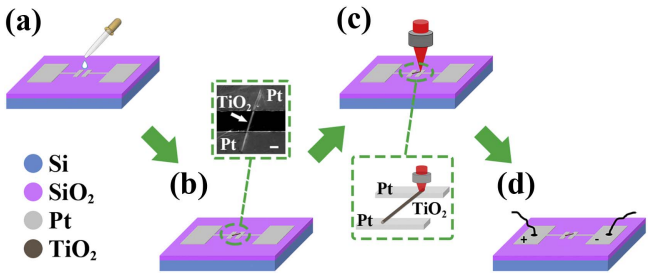

Figure 1. Schematic diagrams showing the assembly process of bridged Pt/TiO_2 NW/Pt structures. (a) Deposition, (b) drying, (c) laser irradiation and (d) under electrical test. The inset in (b) shows an SEM image of the structure as assembled. The scale bar is 1 μm. The inset in (c) shows the detail of the irradiation process.

electrodes which had been previously rinsed with high purity acetone and deionized water, and dried in air. Fs laser pulses (800 nm wavelength and 1 kHz frequency), generated from a Ti: sapphire laser system with 50 fs pulse duration, were used for localized irradiation. An objective lens with numerical aperture =0.5 and long working distance (5 mm) focused the laser beam at normal incidence to a nanoscale spot overlapping a small portion of the NW at the junction, as shown in the inset in figure 1(c), while a mechanical shutter was used to control the laser irradiation time (number of pulses). The fluence at the sample surface was controlled by reflective neutral density filters and by beam defocusing. Electrical properties were measured under the condition of grounding the electrode on the irradiated side.

The morphology and phase identification of TiO_2 NWs were examined by scanning electron microscopy (SEM), transmission electron microscopy (TEM) and x-ray diffraction (XRD). The elemental composition in nanoscale structures were analyzed by nano Auger electron spectroscopy (nano-AES, PHI 700). Electrical characteristics in the voltage sweeping mode at room temperature were measured using a precision source and measuring unit (Agilent B2911A). Commercial software, COMSOL Multiphysics 5.2a with a RF module, was used to simulate the electric field distribution around the Pt/TiO_2 NW/Pt structure in air under polarized Gaussian beam excitation at a wavelength of 800 nm.

3. Results and discussion

Figure 2(a) shows an SEM image of TiO_2 NWs placed on a Si substrate. The diameters of these NWs range from 100–200 nm and their lengths range from 1–8 μm. XRD patterns of TiO_2 NWs indicating the pure rutile phase are shown in figure 2(b). TEM images in figures 2(c) and (d) show the single crystal structure of the NW. The rutile phase is known to occur as a stable high temperature and pressure phase [25]. In addition, metal atoms usually have poor wettability on the surface of an oxide [26]. These characteristics illustrate the effect of laser modification in these experiments.

After depositing TiO_2 NWs on the chip containing Pt electrodes, Pt/TiO_2 NW/Pt structures are ready for processing with fs laser irradiation. Near-field effects are induced at

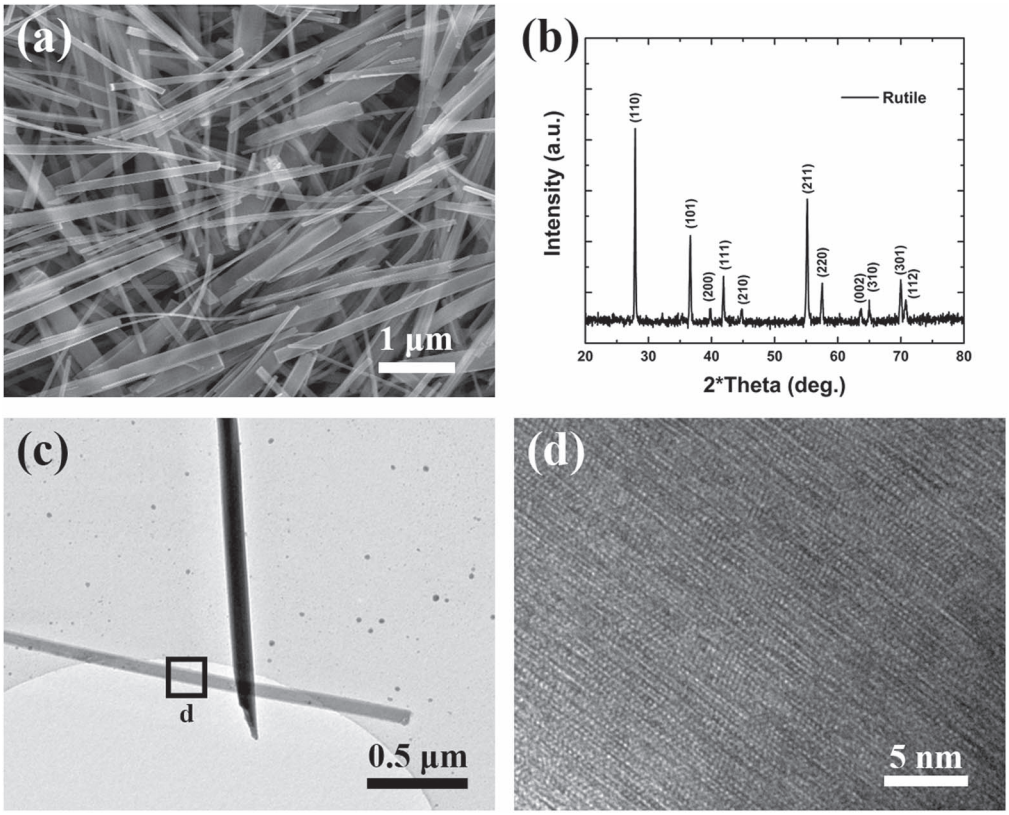

Figure 2. (a) SEM image of as synthesized TiO_2 nanowires. (b) XRD spectrum of TiO_2 after calcination at 900 °C for 2 h. (c) and (d) TEM images of a TiO_2 nanowire.

the Pt/TiO_2 NW interface under irradiation, resulting in an enhancement in the field intensity and plasmon-enhanced optical absorption [27]. The electric field distribution in the Pt/TiO_2 NW interface has been simulated (in air) under two different laser polarizations (figures 3(a) and (b)). The spot size of laser beam is 500 nm, while the diameter of TiO_2 NW is 200 nm. When the polarization direction is parallel to the long axis of the NW, the field enhancement at the metal/oxide interface is clearly visible and is much stronger than that at the oxide/air interface. When the polarization direction is perpendicular to the NW, excitation is seen at both the metal/oxide interface and in part of the oxide/air interface. The electrical field around the NW is notably enhanced near the irradiated region for both polarizations. These results indicate that localized regions in NWs and electrodes can be selectively irradiated by a focused fs laser beam. The simulation shows that the field intensity is also weakly enhanced at the metal/oxide interface on the opposite electrode. This effect can be reduced by controlling the fluence in the fs laser beam.

Figures 3(c)–(e) show SEM images of the Pt/TiO_2 NW structure after fs laser irradiation at different fluences (5.02, 21.7 and 772 mJ cm^{-2}, respectively). Significant ablation and damage to the structure after irradiation at high fluence is shown by the arrow in figure 3(e). However, bonding between the Pt electrode and the TiO_2 NW is apparent after irradiation at low fluence. At intermediate fluence, an enhancement in the optical plasmonic effect at the heterojunction yields damage along the top surface of the TiO_2 NW (figure 3(d)).

To investigate the chemical effects in these materials after localized fs laser irradiation, surface elemental composition (at a depth of $\leqslant$10 nm) around the bond has been analyzed using nano-AES. Two sweep modes were used to get the Auger electron energy spectra. A series of Auger spectra were measured at three different points with an electron beam energy of 10 keV (figures 4(a) and (b)). Using the O 575 $\pm$ 5 eV peak and corresponding sensitivity factors, it can be seen that the oxygen content at location 2 is higher than that at location 1. This implies that the bond at the Pt/TiO_2 NW interface has lower oxygen content than that of the original NW. Although some organic residue occurs when depositing NWs on the chips (see the C peak in the Auger spectra in figure 4(b)), the oxygen content in the location of the bond (Point 1) is higher than that on the Pt electrode (Point 3). Similar results are also obtained along a linear track (figure 4(d)). Prior to fs laser irradiation, an O peak is observed at the center corresponding to the position of the TiO_2 NW in the SEM image (figure 4(c)), while a weak single O peak is shown at the laser-irradiated location.

These results reveal that new compositions, characterized by low oxygen content, are generated between the Pt electrode and the TiO_2 NW after fs laser irradiation. It is expected that a thin Magnéli layer (oxygen deficient TiO_{2-x}) is formed between the Pt electrode and the TiO_2 NW by redox reactions during high intensity excitation [28]. This layer, containing a

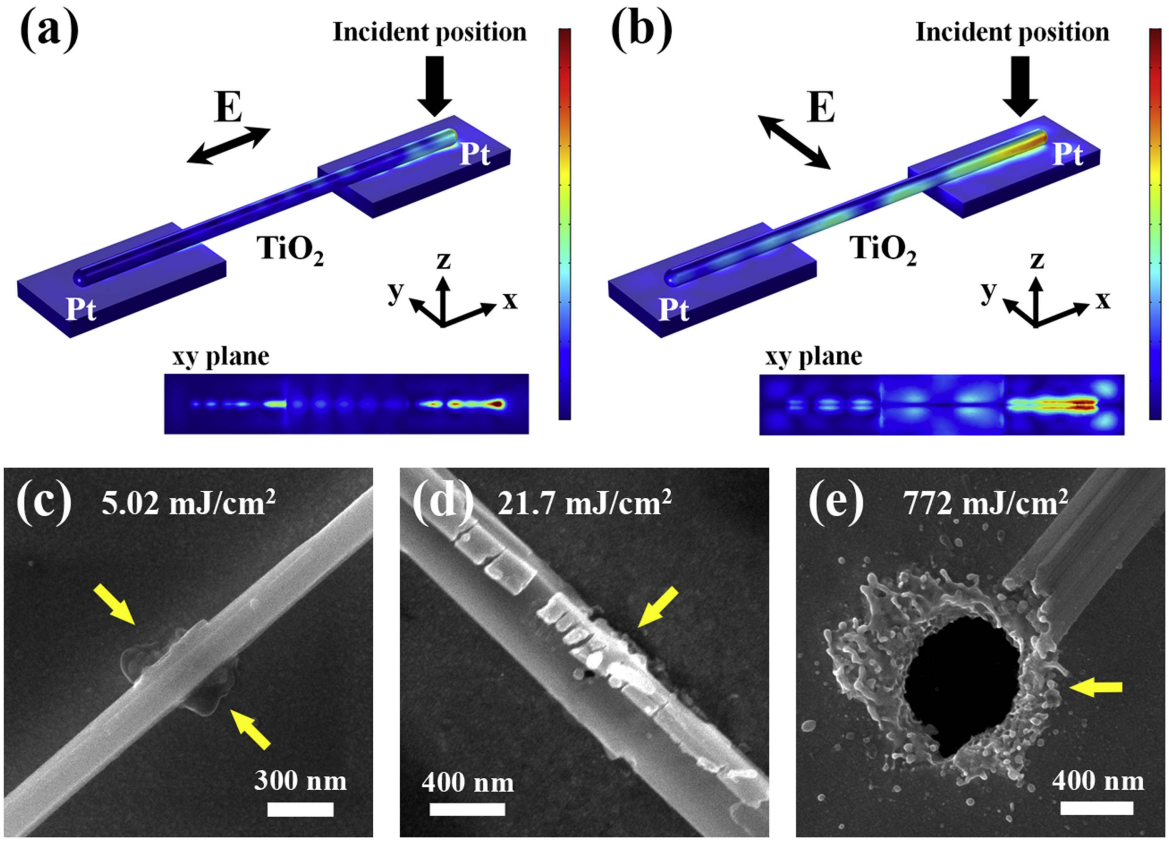

Figure 3. Simulation of the electric field distribution around the Pt/TiO_2 NW interface during irradiation with different polarization of the Gaussian beam: (a) polarization in the *x* direction and (b) polarization in the *y* direction. Insets show the electric field distributions in the *xy* plane in both cases. SEM images of the Pt/TiO_2 NW interface after localized fs laser irradiation at fluences of (c) 5.02, (d) 21.7 and (e) 772 mJ cm^{-2}. Irradiation time: 10 s.

high defect concentration, acts as a connecting bridge between the two components and plays a key role in the modification of the metal/oxide interface. The barrier height of the interface greatly depends on the defect distribution in the TiO_2 NW near the heterojunction [29]. In the experiment, there are few defects inside the TiO_2 NW (see figure 2(d)). Good crystallinity is helpful to keep intrinsic properties of TiO_2 semiconductor. Besides, considering the work function of Pt and TiO_2, a Schottky barrier appears at the Pt/TiO_2 NW junction when depositing the NW on the electrodes due to the weak Van der Waals interaction (figure 4(e)) [30]. Surface plasmons, excited by fs laser irradiation, facilitate bonding between the Pt electrode and the TiO_2 NW, resulting in the formation of new compositions characterized by high defect concentration. Such defects will consist of oxygen vacancies and/or Ti interstitials [28]. Previous studies suggest that these laser-induced defects can reduce the barrier height of the Schottky heterojunction (figure 4(f)), and sometimes even facilitate transformation into an Ohmic contact [31].

In order to study the effects of fs laser irradiation on the interface, *I–V* characteristics of the bridged structures have been measured. Figures 5(a) and (b) show significant changes in this characteristic curve at laser fluences of 5.02 mJ cm^{-2} and 772 mJ cm^{-2}, respectively. In figure 5(a), the voltage sweep goes from +25 to −25 V. In the absence of fs laser irradiation, a self-rectifying characteristic is apparent. An abrupt increase in conductance is observed when the voltage ramps to −20 V. This is then the so-called ON-state-voltage where the current response increases abruptly [32]. After fs laser irradiation, the current response during the voltage sweep is initially small (16 nA) at a bias voltage of 25 V. As the voltage is reduced from 25 V, the current response increases gradually until the voltage reaches 20 V. This increase occurs because ionic conduction in oxide materials is a function of voltage dependent redox reactions and elimination of the reaction products into the air [33, 34]. As the voltage decreases below 20 V, a linear characteristic is found in the *I–V* curve until the voltage reaches 0 V. On application of a reverse bias, the current increases abruptly at about −12 V, which is a response of Schottky contact. The difference of ON-state-voltage before and after laser irradiation indicates the reduction of Schottky barrier [35]. Current instabilities are found at reverse biases exceeding −14 V, due to the Joule heating associated with the high current density (>100 A cm^{-2}) in the NW.

The asymmetric current response with different bias voltage seen after fs laser irradiation (figure 5(a)) indicates that the applied bias voltage influences the barrier height. In the present devices, the Pt/TiO_2 NW/Pt structure can be considered as a pair of reverse biased Schottky diodes. When a bias voltage is applied, one of the Schottky barriers (at the cathode) is always under reverse bias, so that it dominates the

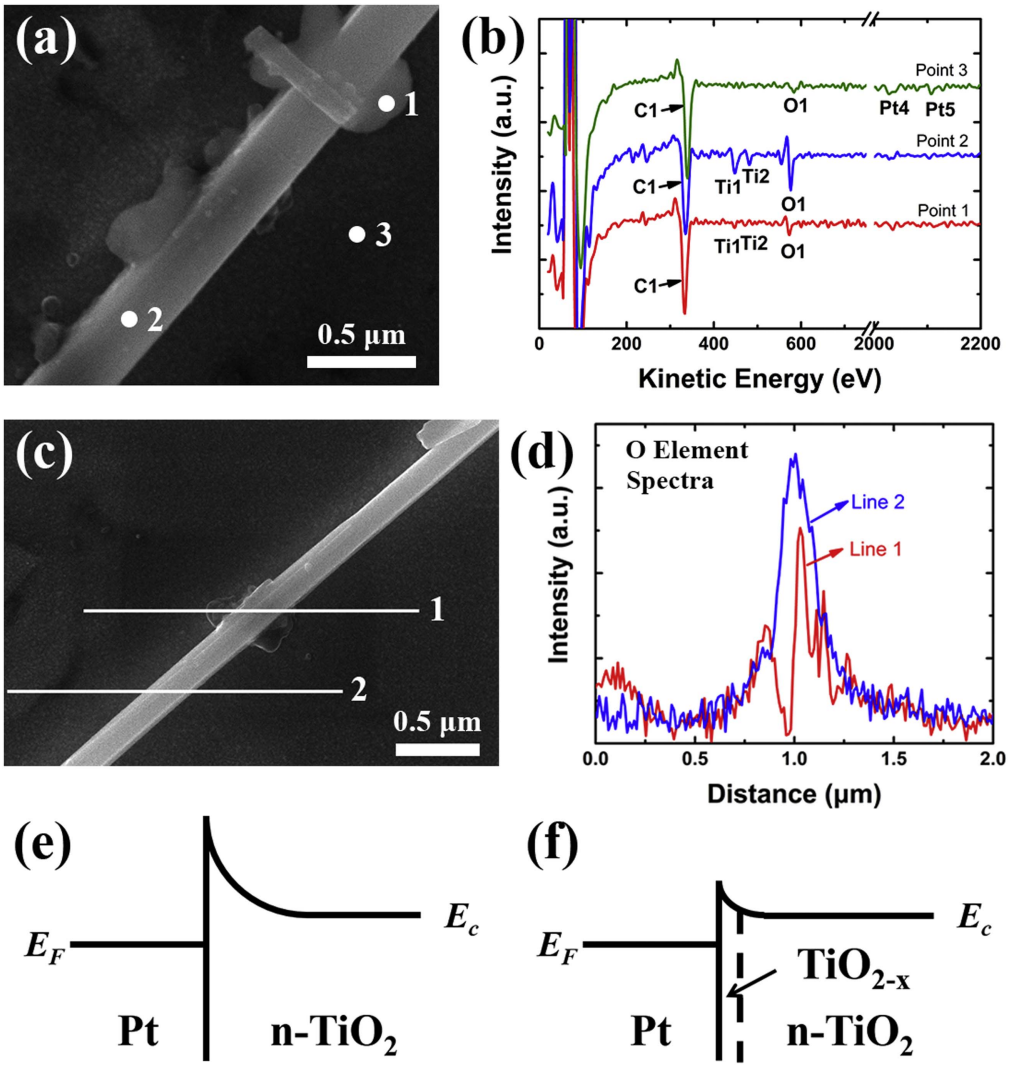

Figure 4. Nano-AES analysis of Pt/TiO_2 NW interfaces. (a) and (c) are SEM images of a TiO_2 NW after laser irradiation at a fluence of 5.02 mJ cm^{-2}. (b) and (d) are the corresponding nano-AES results with point and linear sweeping, respectively. Energy band diagrams showing the relevant states: (e) before laser irradiation and (f) after laser irradiation.

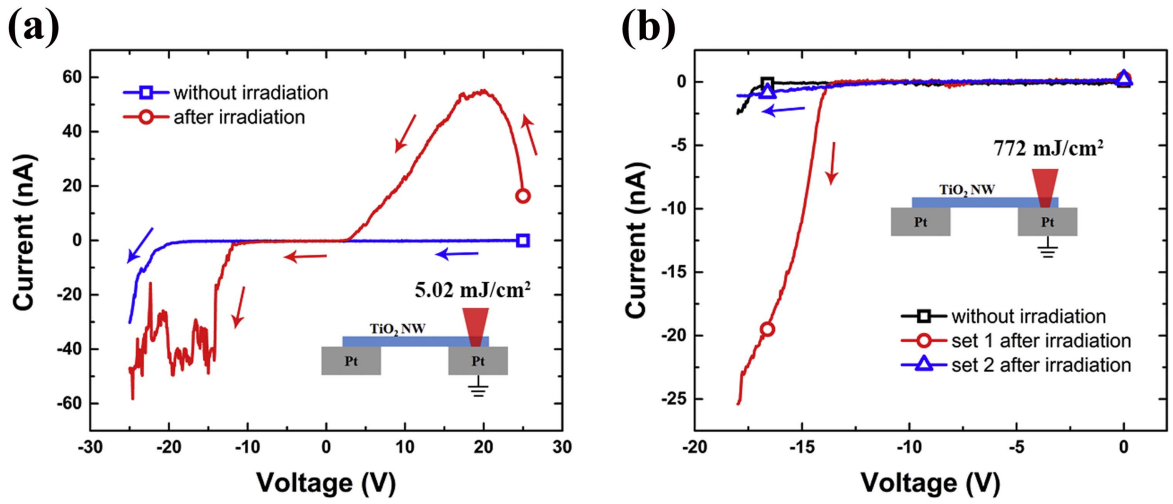

Figure 5. Current response of single TiO_2 nanowire before and after localized fs laser irradiation. Insets show schematic diagrams of the test structure and the locations subjected to laser irradiation. (a) 25 V → −25 V, laser fluence: 5.02 mJ cm^{-2}, irradiation time: 10 s. (b) 0 V → −18 V, laser fluence: 772 mJ cm^{-2}, irradiation time: 1 s.

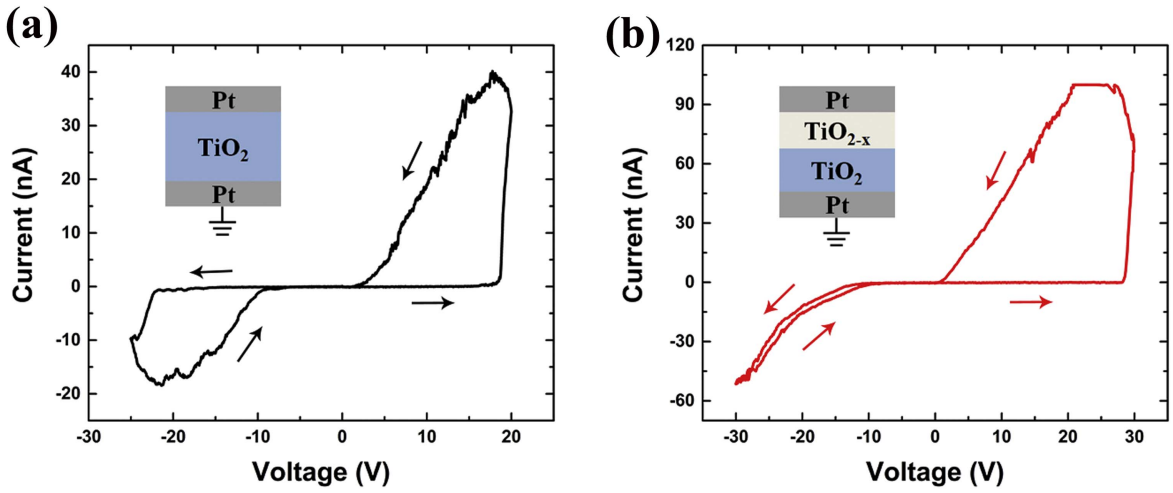

Figure 6. Current response of a single TiO_2 nanowire: (a) in the initial state and (b) after localized fs laser irradiation on the top electrode. The voltage cycle is (a) 0 V → −25 V → 20 V → 0 V and (b) 0 V → −30 V → 30 V → 0 V. Upper insets show schematic diagrams of the composition of bridged structures before and after localized fs laser irradiation.

overall impedance. If the heterojunction at the cathode is modified by fs laser irradiation, the conductivity of the bridged structure is greatly increased. This is reflected in the appearance of a linear *I–V* characteristic.

Figure 5(b) shows the *I–V* characteristic under negative bias of the bridged structure after processing at a laser fluence of 772 mJ cm^{-2}. Before fs laser irradiation, the ON-state-voltage is about −17 V. After fs laser irradiation, the ON-state-voltage changes following different voltage cycles. The irreducible characteristic of the electrical response indicates that the heterojunction is unstable. As noted above, both the TiO_2 NW and the Pt electrode are significantly ablated at high laser fluence resulting in weak bonding between metal and oxide. These low-strength bonds may cause the heterojunction to fail under voltage cycling. The conductivity of the Pt/TiO_2 NW interface is then directly related to the mechanical strength of the junction as reported elsewhere [36].

Experimental data on the elemental composition, and its relation to electrical properties in these devices, suggests that understanding the resistive switching (RS) behavior of the bridged structure will be useful in improving the functionality of TiO_2 memristors. Figure 6(a) shows a typical *I–V* characteristic for such a bridged structure in the initial state. This curve exhibits the hysteresis loop commonly seen in RS devices. The appearance of hysteresis is usually attributed to the accelerated diffusion of oxygen vacancies in response to an applied voltage and the accumulation of these vacancies at the surface [37]. Hysteresis then represents a natural method of storing information in a circuit. To enhance the performance of RS devices, an oxygen-deficient TiO_{2-x} layer is usually introduced on the anode side of the metal/oxide interface by deposition or by electroforming [31, 34]. The current study shows that the same effect can be produced by fs laser irradiation over a localized area. Figure 6(b) shows the current response (voltage cycle 0 V → −30 V → 30 V → 0 V) of bridged structures after localized fs laser irradiation at the anode with a fluence of 5.02 mJ cm^{-2}. Laser irradiation is seen

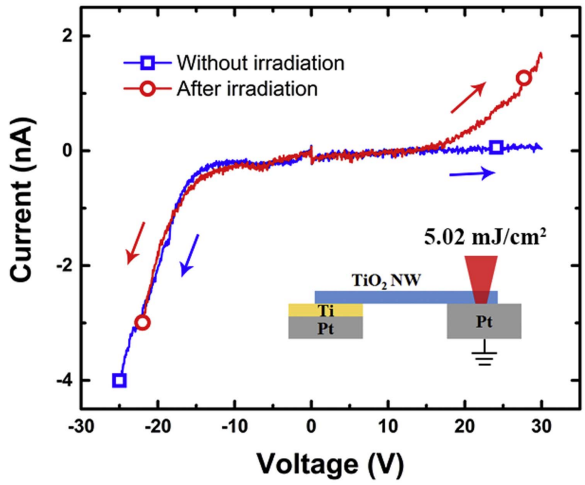

Figure 7. The current response of a single TiO_2 nanowire in a Ti/TiO_2 NW/Pt structure. The voltage scan is 0 V → 30 V and 0 V → − 25 V. The inset shows a schematic diagram of the bridged structure and the irradiated area.

to produce significant changes in the *I–V* response. A primary effect is the absence of a hysteresis characteristic under negative bias, together with a larger high resistance/low resistance ratio under forward bias. Although a hysteresis loop is only observed for the positive voltage sweep, a small negative bias is sufficient to switch the device back to the 'OFF' state [38]. The information storage capability of the device is then enhanced by fs laser irradiation.

A symmetric current response can also be realized by localized fs laser irradiation of an asymmetric bridged structure. Ti and Pt electrodes having the same gap (2 μm) are fabricated and an asymmetric Ti/TiO_2 NW/Pt structure is created by depositing a TiO_2 NW on the chip (figure 7). A thin Ti layer (15 nm thickness) is deposited on top of a 185 nm of Pt layer. This Ti layer must be thin enough to avoid reduction of the TiO_2 NW. Previous studies have demonstrated that an Ohmic contact forms spontaneously when TiO_2

is deposited on a Ti electrode due to chemical reactions at the interface [39]. Although organic residues may prevent the formation of an ideal Ohmic contact in the present experiment, the barrier height in the Ti/TiO_2 NW heterojunction is much smaller than that in the Pt/TiO_2 NW heterojunction. Figure 7 shows *I–V* curves for the new structure under different bias voltages. In all of these measurements, the Pt electrode without the 15 nm Ti-layer is grounded. After fs laser irradiation at the position of this electrode an enhancement of the current from 0.04 to 1.62 nA occurs at forward bias voltage of 30 V. A similar current response is found with a reverse bias. These results confirm that the contact state of the metal/oxide interface changes in response to spatially localized fs laser processing. Laser engineering of contact states in such compositions is then a promising technique for the fabrication of nanoelectronic devices with a characteristic of selective and precise controlling of local composition or interfacial state of materials for different property requirement in practical applications.

4. Conclusion

We have investigated the effect of fs laser-induced modification at the Pt/TiO_2 NW interface in free-standing bridged structures. Nanojoining of a Pt electrode and a TiO_2 NW can be obtained under focused fs laser irradiation at a fluence of 5.02 mJ cm^{-2}. Numerical simulations suggest that strong plasmonic-enhanced electric fields exist at the metal/oxide interface and that these contribute to enhanced bonding. Nano-AES scans indicate that a localized oxygen deficiency in the TiO_2 NW, together with the formation of Magnéli phases, is produced in the region of tightly focused fs laser irradiation. A reduction in the Schottky barrier height and the direction of the applied bias voltage directly influence the current response in these bridged structures. This study shows that optical processing with fs laser irradiation is effective in the generation of asymmetric electrical properties and yields further insight into how laser engineering of the contact state at the metal/oxide interface can used to improve the properties of RS devices.

Acknowledgments

This research is supported by the National Natural Science Foundation of China (51520105007 and 51375261) and the National Key Research and Development Program of China (2017YFB1104900). The author would like to thank PhD student Ming Xiao for fruitful discussions.

References

[1] Zheng D *et al* 2016 When nanowires meet ultrahigh ferroelectric field-high-performance full-depleted nanowire photodetectors *Nano Lett.* **16** 2548–55
[2] Rui Z, Wei P, Qing Z, Yan C, Xuejiao C, Zhihong F, Jianhua Y and Daihua Z 2016 Enhanced non-volatile resistive switching in suspended single-crystalline ZnO nanowire with controllable multiple states *Nanotechnology* **27** 315203
[3] Cao F, Xiong J, Wu F, Liu Q, Shi Z, Yu Y, Wang X and Li L 2016 Enhanced photoelectrochemical performance from rationally designed anatase/rutile TiO_2 heterostructures *ACS Appl. Mater. Interfaces* **8** 12239–45
[4] Zhang D, Gu X, Jing F, Gao F, Zhou J and Ruan S 2015 High performance ultraviolet detector based on TiO_2/ZnO heterojunction *J. Alloys Compd.* **618** 551–4
[5] Timko B P, Cohen-Karni T, Yu G, Qing Q, Tian B and Lieber C M 2009 Electrical recording from hearts with flexible nanowire device arrays *Nano Lett.* **9** 914–8
[6] Han J-W, Rim T, Baek C-K and Meyyappan M 2015 Chemical gated field effect transistor by hybrid integration of one-dimensional silicon nanowire and two-dimensional tin oxide thin film for low power gas sensor *ACS Appl. Mater. Interfaces* **7** 21263–9
[7] Liang K-D, Huang C-H, Lai C-C, Huang J-S, Tsai H-W, Wang Y-C, Shih Y-C, Chang M-T, Lo S-C and Chueh Y-L 2014 Single CuO_x nanowire memristor: forming-free resistive switching behavior *ACS Appl. Mater. Interfaces* **6** 16537–44
[8] Perea D E, Hemesath E R, Schwalbach E J, Lensch-Falk J L, Voorhees P W and Lauhon L J 2009 Direct measurement of dopant distribution in an individual vapour–liquid–solid nanowire *Nat. Nanotechnol.* **4** 315–9
[9] Nagashima K, Yanagida T, Oka K, Taniguchi M, Kawai T, Kim J-S and Park B H 2010 Resistive switching multistate nonvolatile memory effects in a single cobalt oxide nanowire *Nano Lett.* **10** 1359–63
[10] Huang Y, Duan X, Cui Y and Lieber C M 2002 Gallium nitride nanowire nanodevices *Nano Lett.* **2** 101–4
[11] Zhang K, Ravishankar S, Ma M, Veerappan G, Bisquert J, Fabregat-Santiago F and Park J H 2017 Overcoming charge collection limitation at solid/liquid interface by a controllable crystal deficient overlayer *Adv. Energy Mater.* **7** 1600923
[12] Huang Y, Duan X and Lieber C M 2005 Nanowires for integrated multicolor nanophotonics *Small* **1** 142–7
[13] Zhang Q, Li G, Liu X, Qian F, Li Y, Sum T C, Lieber C M and Xiong Q 2014 A room temperature low-threshold ultraviolet plasmonic nanolaser *Nat. Commun.* **5** 4953
[14] Wang G, Wang H, Ling Y, Tang Y, Yang X, Fitzmorris R C, Wang C, Zhang J Z and Li Y 2011 Hydrogen-treated TiO_2 nanowire arrays for photoelectrochemical water splitting *Nano Lett.* **11** 3026–33
[15] Zhu K, Neale N R, Miedaner A and Frank A J 2007 Enhanced charge-collection efficiencies and light scattering in dye-sensitized solar cells using oriented TiO_2 nanotubes arrays *Nano Lett.* **7** 69–74
[16] Cai X, Wu H, Hou S, Peng M, Yu X and Zou D 2014 Dye-sensitized solar cells with vertically aligned TiO_2 nanowire arrays grown on carbon fibers *ChemSusChem* **7** 474–82
[17] Zhang J, Zhou P, Liu J and Yu J 2014 New understanding of the difference of photocatalytic activity among anatase, rutile and brookite TiO_2 *Phys. Chem. Chem. Phys.* **16** 20382–6
[18] Wang Y *et al* 2016 A self-powered fast-response ultraviolet detector of p–n homojunction assembled from two ZnO-based nanowires *Nano-Micro Lett.* **9** 11
[19] Nam C Y, Tham D and Fischer J E 2005 Disorder effects in focused-ion-beam-deposited Pt contacts on GaN nanowires *Nano Lett.* **5** 2029–33
[20] George A, Knez M, Hlawacek G, Hagedoorn D, Verputten H H J, van Gastel R and ten Elshof J E 2012 Nanoscale patterning of organosilane molecular thin films from the gas phase and its applications: fabrication of

multifunctional surfaces and large area molecular templates for site-selective material deposition *Langmuir* **28** 3045–52
[21] Herzer N, Hoeppener S and Schubert U S 2010 Fabrication of patterned silane based self-assembled monolayers by photolithography and surface reactions on silicon-oxide substrates *Chem. Commun.* **46** 5634–52
[22] Keller U 2003 Recent developments in compact ultrafast lasers *Nature* **424** 831–8
[23] Liu L, Peng P, Hu A, Zou G, Duley W W and Zhou Y N 2013 Highly localized heat generation by femtosecond laser induced plasmon excitation in Ag nanowires *Appl. Phys. Lett.* **102** 073107
[24] Hu A, Zhang X, Oakes K D, Peng P, Zhou Y N and Servos M R 2011 Hydrothermal growth of free standing TiO_2 nanowire membranes for photocatalytic degradation of pharmaceuticals *J. Hazardous Mater.* **189** 278–85
[25] Bai J and Zhou B 2014 Titanium dioxide nanomaterials for sensor applications *Chem. Rev.* **114** 10131–76
[26] Eustathopoulos N and Drevet B 1998 Determination of the nature of metal-oxide interfacial interactions from sessile drop data *Mater. Sci. Eng.* A **249** 176–83
[27] Maier S A and Atwater H A 2005 Plasmonics: localization and guiding of electromagnetic energy in metal/dielectric structures *J. Appl. Phys.* **98** 011101
[28] Nakajima T, Tsuchiya T and Kumagai T 2009 Pulsed laser-induced oxygen deficiency at TiO_2 surface: anomalous structure and electrical transport properties *J. Solid State Chem.* **182** 2560–5
[29] Lin L, Zou G, Liu L, Duley W W and Zhou Y N 2016 Plasmonic engineering of metal-oxide nanowire heterojunctions in integrated nanowire rectification units *Appl. Phys. Lett.* **108** 203107
[30] Mrovec M, Albina J M, Meyer B and Elsässer C 2009 Schottky barriers at transition-metal/$SrTiO_3$(001) interfaces *Phys. Rev.* B **79** 245121
[31] Yang J J, Pickett M D, Li X, OhlbergDouglas A A, Stewart D R and Williams R S 2008 Memristive switching mechanism for metal/oxide/metal nanodevices *Nat. Nanotechnol.* **3** 429–33
[32] Wang M-Z, Liang F-X, Nie B, Zeng L-H, Zheng L-X, Lv P, Yu Y-Q, Xie C, Li Y Y and Luo L-B 2013 TiO_2 nanotube array/monolayer graphene film Schottky junction ultraviolet light photodetectors *Part. Part. Syst. Charact.* **30** 630–6
[33] Moballegh A and Dickey E C 2015 Electric-field-induced point defect redistribution in single-crystal TiO_{2-x} and effects on electrical transport *Acta Mater.* **86** 352–60
[34] Jeong D S, Schroeder H, Breuer U and Waser R 2008 Characteristic electroforming behavior in Pt/TiO_2/Pt resistive switching cells depending on atmosphere *J. Appl. Phys.* **104** 123716
[35] Park J, Song H, Lee E K, Oh J H and Yong K 2015 ZnO nanowire based photoelectrical resistive switches for flexible memory *J. Electrochem. Soc.* **162** H713–8
[36] Lin L, Liu L, Musselman K, Zou G, Duley W W and Zhou Y N 2016 Plasmonic-radiation-enhanced metal oxide nanowire heterojunctions for controllable multilevel memory *Adv. Funct. Mater.* **26** 5979–86
[37] Wu W and Wang Z L 2011 Piezotronic nanowire-based resistive switches As programmable electromechanical memories *Nano Lett.* **11** 2779–85
[38] Strukov D B, Snider G S, Stewart D R and Williams R S 2008 The missing memristor found *Nature* **453** 80–3
[39] Hernández-Rodríguez E, Márquez-Herrera A, Zaleta-Alejandre E, Meléndez-Lira M, Cruz W D L and Zapata-Torres M 2013 Effect of electrode type in the resistive switching behaviour of TiO_2 thin films *J. Phys. D: Appl. Phys.* **46** 045103